Zeitschrift: IABSE reports of the working commissions = Rapports des commissions de travail AIPC = IVBH Berichte der Arbeitskommissionen

Band: 34 (1981)

Artikel: Nonlinear analysis of a prestressed concrete bridge

Autor: Ketchum, Mark A. / Scordelis, Alex C.

DOI: https://doi.org/10.5169/seals-26915

Nonlinear Analysis of a Prestressed Concrete Bridge

Analyse non-linéaire d'un pont en béton précontraint

Nichtlineare Berechnung einer Spannbetonbrücke

MARK A. KETCHUM
Research Assistant
University of California
Berkeley, California, USA

ALEX C. SCORDELIS
Professor of Civil Engineering
University of California
Berkeley, California, USA

SUMMARY

A nonlinear material and time dependent analysis is applied to a three span continuous post tensioned single cell concrete box girder bridge. The analytical procedure, based on the finite element method, considers the nonlinear stress strain relationships of the materials as well as the time dependent effects of creep, shrinkage, relaxation of prestress, and load history. The time dependent behavior of the bridge is traced through a period of 27 years from the time of construction. Overload behavior and ultimate strength under increasing vehicular load are investigated at two times in the service life of the bridge. The bridge is shown to have a large overload capacity.

RÉSUMÉ

Une analyse de type non-linéaire et dépendant du temps est appliquée à un ouvrage à trois travées continues formé d'un caisson en béton précontraint. L'analyse, basée sur la méthode des éléments finis, prend en compte la relation non linéaire contrainte-déformation des matériaux ainsi que les effets du fluage, du retrait, de la relaxation des aciers et du processus de chargement. Le comportement de l'ouvrage est suivi sur 27 années s'écoulant après sa finition, en particulier sous charges ultimes, appliquées deux fois pendant cette période. Il se révèle que l'ouvrge a une large résistance résiduelle vis-à-vis des surcharges.

ZUSAMMENFASSUNG

Eine dreifeldrige, durchlaufende, einzellige Hohlkastenspannbetonbrücke wird unter Berücksichtigung von nichtlinearem Material- und zeitabhängigem Verhalten berechnet. Das Berechnungsmodell, das auf der Finiten-Elemente-Methode basiert, berücksichtigt sowohl das nichtlineare Spannungs-Dehnungsverhalten des Materials als auch die zeitabhängigen Einflüsse der Belastungsfolge, des Kriechens und Schwindens des Betons und der Relaxation des Spannstahls. Das zeitabhängige Verhalten der Brücke wird über einen Abschnitt von 27 Jahren nach der Bauwerksfertigstellung verfolgt. Das Verhalten unter Überlastung und die maximale Tragfähigheit infolge zunehmender Verkehrslasten sind für zwei Zeitpunkte innerhalb des Nutzungszeitraums der Brücke untersucht. Es wird gezeigt, dass die Brücke eine grosse Überlastkapazität besitzt.

1. INTRODUCTION

Post tensioned concrete box girders are frequently used as structural elements in modern bridge construction. Such highway structures in the United States are currently subjected to increasing truck loads and traffic densities. Design procedures, however, do not always reflect this situation. Some standard design specifications are still based on light weight trucks and outmoded bridge structure types [1]. Recent studies within the California Department of Transportation [2] have indicated a need for explicit consideration of increasing traffic loads and an improved understanding of overload behavior of modern highway structures. Such understanding is also complicated by the time dependent nature of the problem.

In this paper, a post tensioned concrete box girder highway bridge is investigated using a material and time dependent nonlinear analysis, in order to determine its response to time dependent effects and to increasing truck overloads up to ultimate failure. The objectives of the investigation were to use a special purpose finite element computer program for the material, geometric and time dependent analysis of prestressed concrete frames to (1) make a comparison of time dependent response as analytically predicted with that predicted using typical design assumptions and (2) to study the ultimate strength of the structure under increasing truck overloads, both before and after consideration of time dependent response. Results are presented which demonstrate bridge response parameters which include deflections, stresses and their resultants, and strains and curvatures, under these conditions.

2. THE ANALYSIS PROCEDURE

2.1 General

The analytical formulation used for this study has been developed by Kang [3] to trace the material and geometric nonlinear response of reinforced and prestressed concrete planar frames through the elastic, cracking, inelastic, and ultimate ranges. The formulation is implemented in the finite element computer program PCFRAME which is capable of the analysis of planar frames with arbitrary geometry, consisting of beam elements of arbitrary cross section but with a plane of symmetry common to the plane of the structure, Fig. 1. Major goals in the preparation of the computer program included the development of simple but realistic material models for the concrete and steel, their implementation in an efficient discretization of the structural system which captures the significant response of a range of structures of interest, and the development and testing of a reliable and cost effective nonlinear solution algorithm. The detailed theoretical formulation, as well as a comparison of results with those of experimental studies has been reported elsewhere by Kang [4], demonstrating the validity of the nonlinear material, geometric, and time dependent response of concrete beams and planar frames. A brief summary of the theory will be presented here.

2.2 Material Models

The constitutive relationship for concrete includes the effects of creep, shrinkage, aging, and temperature strains. Total uniaxial concrete strain $\varepsilon(t)$ at a time t is assumed to be composed of the following contributions:

$$\varepsilon(t) = \varepsilon^{m}(t) + \varepsilon^{c}(t) + \varepsilon^{s}(t) + \varepsilon^{a}(t) + \varepsilon^{T}(t) \qquad (1)$$

The mechanical strain $\varepsilon^m(t)$ is the instantaneous strain caused by the loads. The nonmechanical strain is assumed to consist of creep strain $\varepsilon^c(t)$, shrinkage strain $\varepsilon^s(t)$, aging strain $\varepsilon^a(t)$ and temperature strain $\varepsilon^t(t)$. Implicit in this formulation is the assumption that the principal of superposition is valid, and that each component of strain can be considered separately. The meanings of these strain components are shown in Fig. 2.

The stress-strain curve for concrete is assumed to be independent of the nonmechanical strain but is influenced by the change with time of the strength and initial elastic modulus of the concrete. This stress-mechanical strain curve considers unloading and reloading but does not consider dynamic cyclic effects. The following assumptions are made in the development of the stress-mechanical strain law: (1) stress is uniaxial; (2) the ascending initial curve is a parabola as proposed by Hognestad [5]; (3) unloading modulus equals the initial modulus; (4) tensile cracking occurs at a limiting value of stress; (5) compression failure occurs at a limitng value of mechanical strain; (6) once cracked, concrete can not again resist tensile stress, but can resist compressive stress upon crack closure and reloading. The resulting stress-strain curve is shown in Fig. 3, and eleven distinct material states are identified.

All concrete properties may vary with time according to the recommendations of ACI Committee 209 [6], based on the work by Branson et al. [7]. In addition, other guidelines such as those of CEB/FIP [8] or Bazant and Panula [9] may be separately input into the computer program if desired.

Creep strains are evaluated based on an age and temperature dependent integral formulation. Creep strain is expressed as a functional of stress σ according to the integral

$$\varepsilon^c(t) = \int_0^t c\left(\tau, t-\tau, T\right) \frac{\partial \sigma(\tau)}{\partial \tau} \, d\tau \tag{2}$$

in which the kernel function $c(\tau, t-\tau, T)$ is the age and temperature dependent specific creep, defined as the creep strain at time t due to a unit sustained stress applied at time τ and temperature T. This kernel is expressed as a series

$$c\left(\tau, t-\tau, T\right) = \sum_{i=1}^{3} \alpha_i(\tau) \left[1 - e^{-\lambda_i \phi(T)(t-\tau)}\right] \tag{3}$$

in which $\alpha_i(\tau)$ and λ_i are coefficients determined by a least squares fit to experimental data, or to specified empirical design curves [7,8,9], and $\phi(T)$ is a temperature shift function [10]. Nonlinear creep at high stress levels is accounted for by the concept of effective stress [11].

Shrinkage strain increments, as well as current concrete strength, are provided as program input explicitly at each stage of the analysis. Shrinkage and aging strains are evaluated on the basis of this information.

Reinforcing steel is represented by a simple bilinear nondegrading hysteretic stress-strain curve, Fig. 4. Four distinct material states can be identified: (1) primary tension or compression; (2) yielded, (3) in load reversal; (4) failed. Thermal strain is the only nonmechanical strain considered for reinforcing steel.

Prestressing steel is represented by a multilinear stress-strain curve, and is assumed to act only in tension. The load reversal modulus is assumed equal to

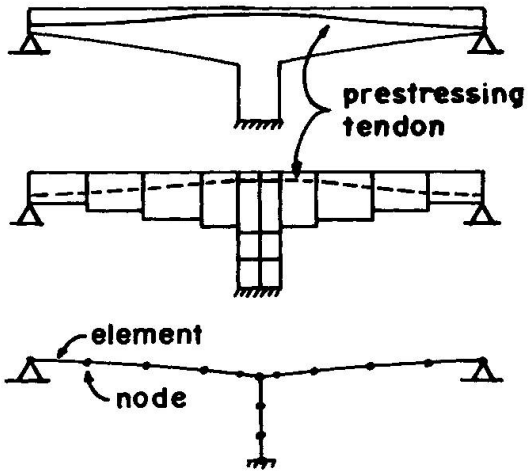

FIG. 1 ACTUAL AND IDEALIZED PRESTRESSED CONCRETE FRAME

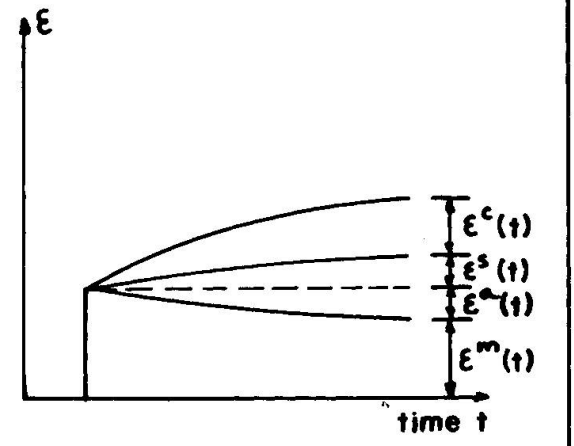

FIG. 2 STRAIN COMPONENTS OF CONCRETE

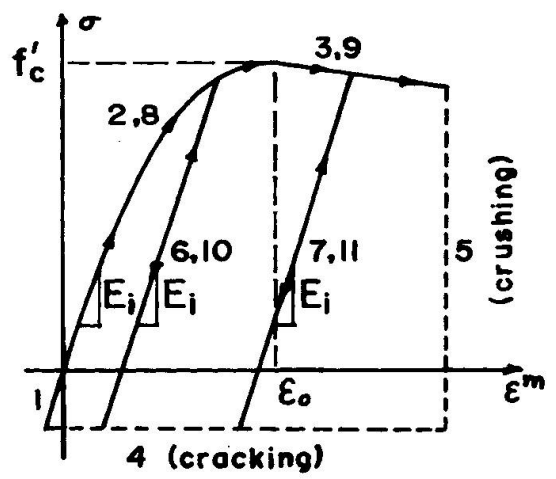

FIG. 3 STRESS-STRAIN CURVE OF CONCRETE

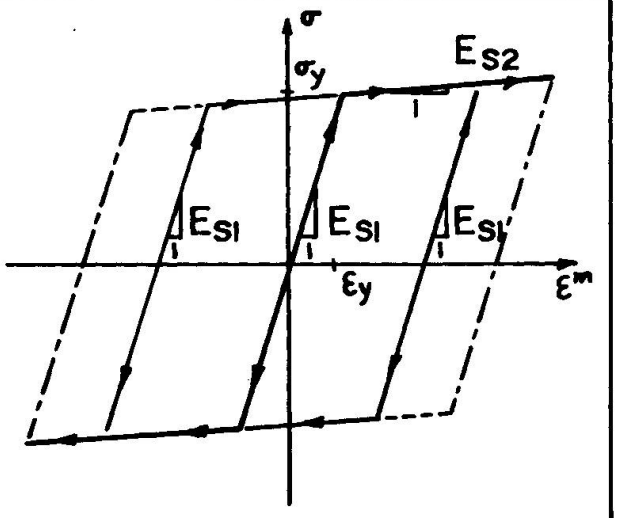

FIG. 4 STRESS-STRAIN CURVE OF MILD STEEL

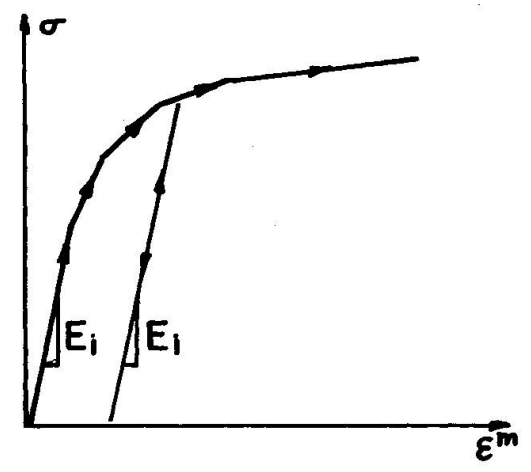

FIG. 5 STRESS-STRAIN CURVE OF PRESTRESSING STEEL

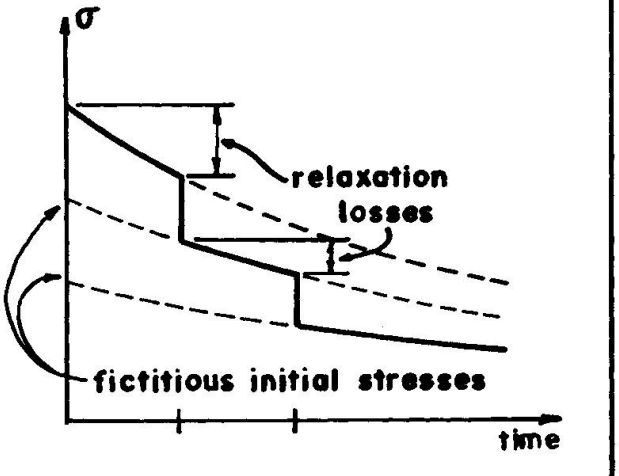

FIG. 6 STRESS RELAXATION OF PRESTRESSING STEEL

the initial modulus, Fig. 5. Stress relaxation is computed utilizing a formula developed by Magura, Sozen, and Seiss [12] and modified for time dependent strains by Hernandez and Gamble [13]. Based on the known time dependent strain variations, a fictitious initial tensioning stress is calculated so that the logarithmic relaxation curve may be applied and result in the correct current stress and relaxation rate. This is shown conceptually in Fig. 6.

2.3 Structural Model

Structural discretization is based on the displacement finite element method, in which the planar structure is idealized as an sssemblage of one dimensional beam finite elements interconnected by nodes, Fig. 1. The cross section is divided into layers, Fig. 7. Element property matrices are evaluated in local element coordinate systems, transformed to the common global system, and then assembled by the direct stiffness method. In a geometrically nonlinear analysis, the local coordinate systems are assumed to change according to the current deformed state of the structure.

The layered finite element, Fig. 7, is assumed to be prismatic, and must have an axis of symmetry in the plane of the structure. This six degree of freedom element represents the entire width and a portion of the length of the bridge girder or other structural element, thus shear lag, as well as torsion and associated warping and distortion of the box girder cross section are neglected in this study. The composite layer system consisting of a finite number of discrete concrete and steel layers is adopted to account for the varied materials and material states across the depth of an element. Each layer is assumed to be in a state of uniaxial stress, and its geometry is completely described by its area and local y-coordinate. A prestressing steel segment is defined by its end eccentricities, area, and initial force. Friction is considered in the calculation of the initial force. After bonding of a tendon, it is represented by a steel layer to account for its contribution to structural stiffness.

The displacement field within an element is developed by assuming a linear variation of axial displacements and a cubic variation of transverse displacements between the nodes. Thus the classical elementary beam functions are used. Then, adopting Navier's plane section hypothesis, the axial displacement and thus the strain in any layer may be determined. Integration of the terms in the element characteristic matrices is performed on a layer by layer midpoint rule basis over the element depth, and with three point Gauss quadrature along the element length. This and the element shape functions constrain the element to linear curvature. Nonlinear geometry effects, when included, are based on the updated Lagrangian approach.

2.4 Time Dependent Nonlinear Analysis Procedure

The time dependent nonlinear analysis is performed by dividing the time domain into a discrete number of time steps, and discretizing the load, temperature, and shrinkage history accordingly. Then a step forward integration is performed in which incremental solutions are superposed to obtain the current solution. To progress from a solution at time t_{n-1} to time t_n, the nodal load increment is summed from the equivalent loads due to nonmechanical strains, the external joint load increment, and the unbalanced load left over from previous steps. The nonlinear equilibrium equations are solved for this load vector based on an incremental load technique combined with tangent stiffness iteration. Three criteria are used for termination of iteration: (1) unbalanced load tolerance, (2) incremental displacement ratio tolerance, and (3) maximum number of iterations. Output may be printed at each iteration, or only at the end of iteration within the load increment. At the end of the last load increment for

a given time step, the procedure continues to the next time step, or else terminates.

3. DESCRIPTION OF THE BRIDGE STRUCTURE

3.1 Structural Design

The bridge structure considered in this investigation, Fig. 8, is a three span, straight, continuous, post tensioned single cell box girder. Its span arrangement is 48.8 m, 61 m, 48.8 m (160 ft, 200 ft, 160 ft) and its roadway width is 10.4 m (34 ft). Cast-in-place construction is assumed to proceed for the entire structure simultaneously. This is typical for a moderate span two lane highway bridge built in California. Simple support conditions are assumed at the ends of the structure, and vertical bearing supports (not monolithic construction) are assumed at the intermediate columns.

For the sake of simplicity the cross-section, Fig. 8, is assumed constant from end to end of the structure, although design practice often calls for thickening of the bottom slab or the webs in regions near supports. The top slab design is based on the use of transverse post tensioning, although its effects are not considered in this analytical investigation. For ease of discretization of the box girder section into the discrete layer system required for the nonlinear analysis, the top and bottom slabs have been simplified to the uniform thicknesses shown.

Structural design of the girder is based on State of California standard criteria. Concrete strength, mild steel strength, and post tensioning strand strength are assumed to be 27.6 MPa (4000 psi), 413.7 MPa (60,000 psi), and 1861.7 MPa (270,000 psi) respectively. Post tensioning force is proportioned on the basis of a traffic load consisting of a chain of 320 kN (36 ton) trucks in each lane, an impact factor based on span length, and no tension allowed in the concrete after all prestressing force losses have occurred. A total of 8, 31 strand tendons are required, for a total steel area of 244.8 cm^2 (37.94 in^2). Ultimate strength load factor design additionally considers the overload of a 952 kN (107 ton), 33 m (108 ft) long permit vehicle with 13 axles. Mild steel reinforcement, having a total area of 542 cm^2 984 in^2) was uniformly distributed over the cross section. This steel, not required for strength is provided for construction purposes.

3.2 Finite Element Model

For the purpose of this analysis, the bridge is divided into 16 elements, making use of symmetry so that only one half of the length of the bridge is considered. The finite element mesh is shown in Fig. 9.

The cross section is discretized into ten concrete layers as shown in Fig. 10. Since torsion is not considered in the planar frame analysis, the two webs of the box girder are combined into one web with six layers in the model. The top and bottom slabs are each divided into two layers so that partial cracking or crushing can be traced.

This model is utilized to study both the time dependent behavior and the overload behavior of the bridge structure. The time dependent analysis traces the response of the bridge from its initial prestressing through a period of 27 years. The effects of variation of time step size, and the influence of the presence of nominal mild steel reinforcement are studied. Time dependent variation of deflections, curvatures, moments, and stresses as well as prestressing forces are traced. The ultimate load analysis traces the response of the bridge

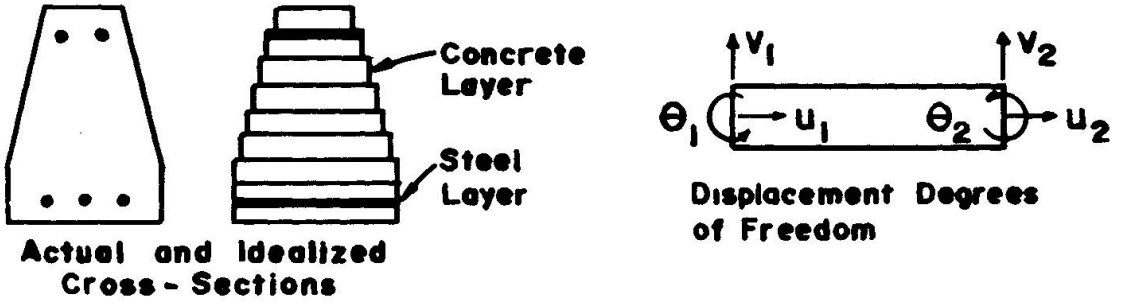

FIG. 7 LAYERED PLANAR BEAM FINITE ELEMENT

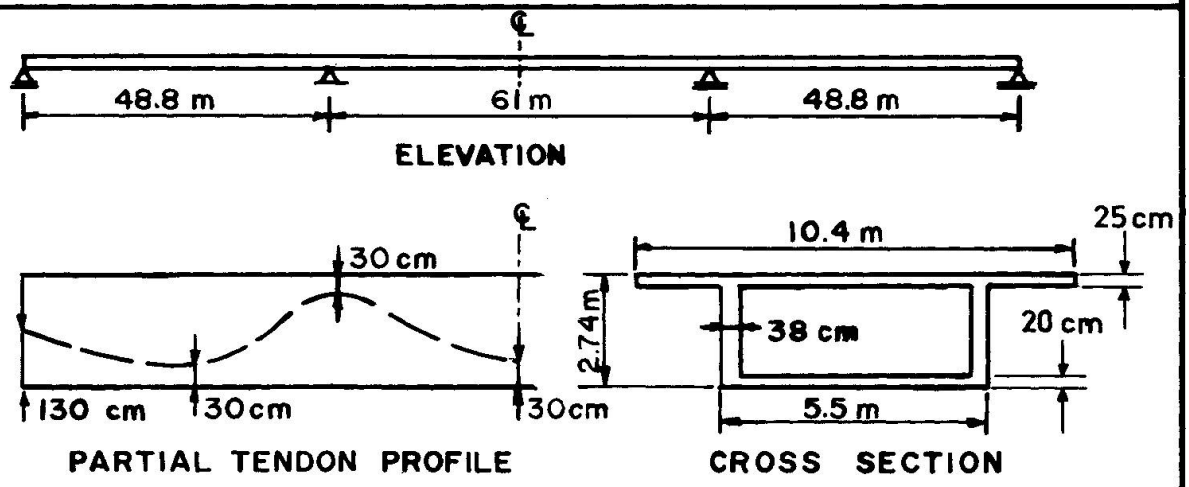

FIG. 8 CONTINUOUS POST TENSIONED CONCRETE SINGLE CELL BOX GIRDER BRIDGE

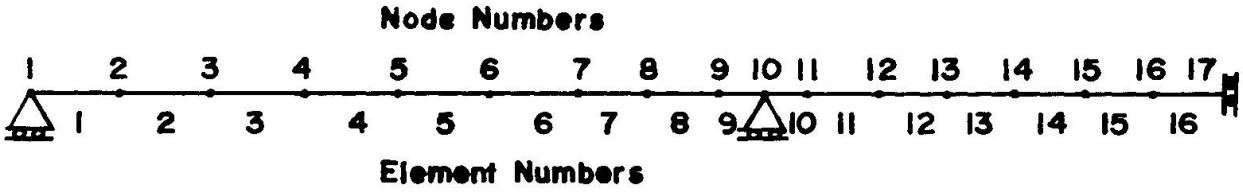

FIG. 9 FINITE ELEMENT MESH OF BRIDGE GIRDER

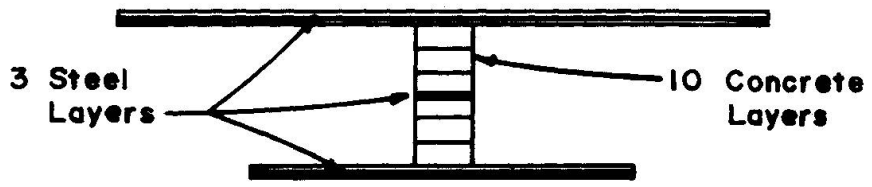

FIG. 10 CROSS SECTION DISCRETIZATION

under increasing loads in the pattern of the California standard overload vehicle previously described. Response curves are presented for increasing loading to ultimate both early in the life of the structure, and after 27 years of time dependent effects have taken place.

4. TIME DEPENDENT ANALYSIS

4.1 Description of Problem

A time dependent analysis of the bridge was performed to determine its response over a 10,000 day (27 year) period with initial loading at 28 days. Intermittent live loads are assumed to play an insignificant role in the time dependent behavior of the structure, therefore the self weight of the girder, and additional dead load due to concrete guard rails, etc. are the only external loads applied to the analytical model. Prestressing is included, considering friction and anchor set losses, generated within the program. Two analytical models are considered, one neglecting the nominal mild steel construction reinforcement, the other including this steel in three discrete layers.

The 10,000 day time period is divided into eight time steps in order to trace the variation of response with time and to provide a basis for a precise solution with the previously described algorithm. The relative lengths of the unequal time steps were chosen in order for creep strains to be of similar magnitude in each time step. Initial creep strain rates are high, so time steps during this period are quite short. Later time steps are made quite long with little or no effect on the solution. Time step size and the creep function are shown in Fig. 11. Longer initial time steps significantly changed the computed response due to the rapid change in the creep function in this time period. Further refinement of the time step size had only a small effect.

Material properties are assumed to be time invariant, thus aging strains are neglected. Strength and initial elastic modulus are taken as 27.6 MPa (4000 psi) and 24856 MPa (3605000 psi) respectively, in accordance with ACI recommendations [6]. An ultimate creep coefficient of 2.5 and ultimate shrinkage strain of 0.001 are utilized, based on a dry climate. Shrinkage is taken as uniform across the depth of the girder.

4.2 Results for Displacement

Figures 12, 13 and 14 present the time variation of displacement response at several locations along the girder. In each figure, response is shown for the two different structural models, one including the nominal mild steel reinforcement, the other neglecting this steel. Time variation of vertical displacement at the middle of the center span of the bridge (Fig. 12), horizontal displacement at the interior support (Fig. 13), and rotation of the interior support (Fig. 14) all show similar trends. Notably evident is the significantly stiffer response of the model including the nominal mild steel reinforcement, both in terms of initial displacement as well as increase in displacement with time. The stiffer initial response agrees well with predictions from an elastic beam theory analysis, based on gross section properties or transformed section properties respectively. Additionally, the model including nominal mild steel reinforcement shows a ratio of 10000 day displacement to initial displacement which is about 20 to 25 percent lower than that for the model without mild steel reinforcement, depending on the displacement component considered. The decrease in creep and shrinkage strain rate as time progresses is also evident in these figures. Displacement increases by a factor of about 3 within the first 100 days, while at 10000 days the response has levelled off so that little additional displacement occurs.

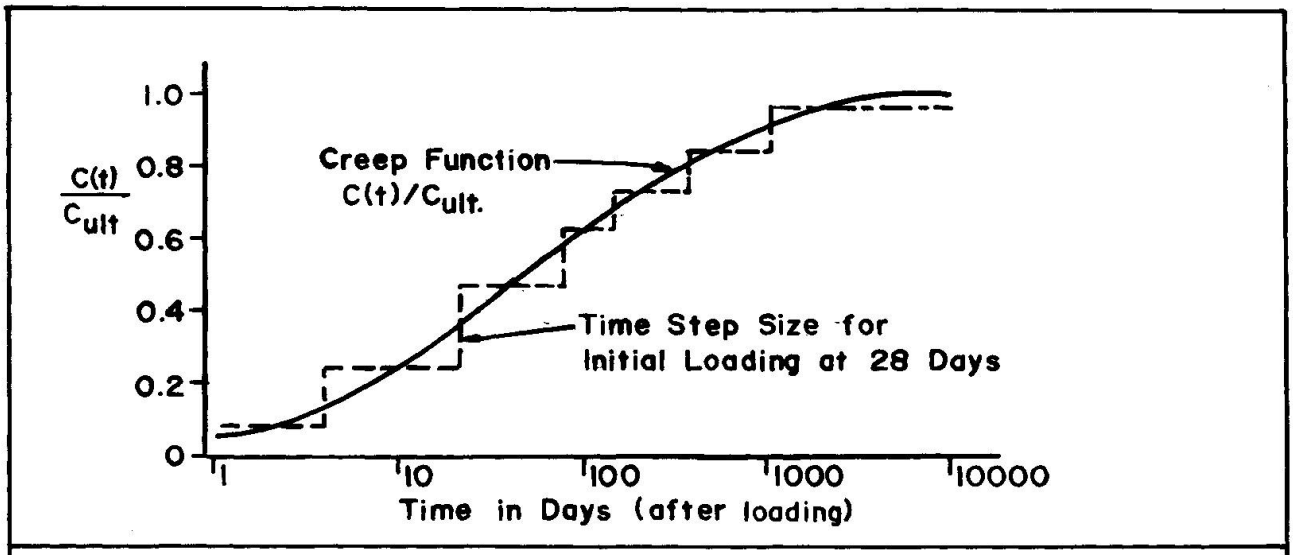

FIG. 11 CREEP FUNCTION AND TIME STEP SIZE

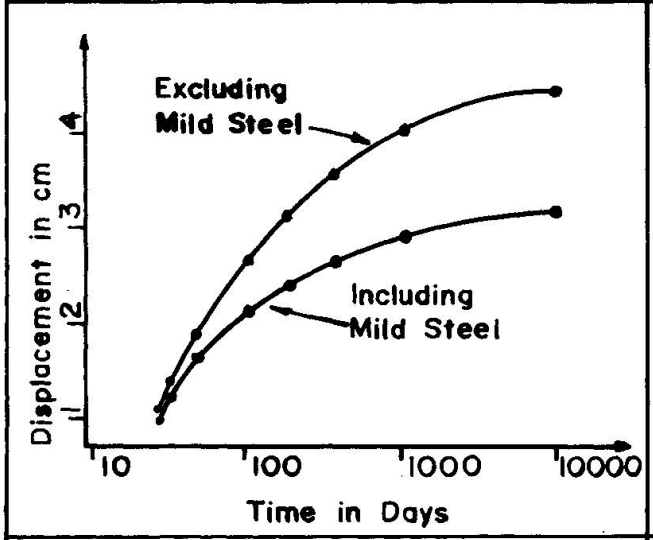

FIG. 12 VERTICAL DISPLACEMENT AT CENTER SPAN VS TIME

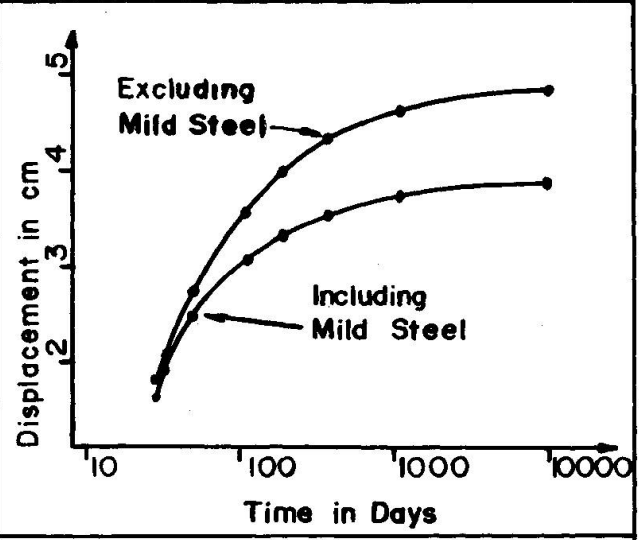

FIG. 13 HORIZONTAL DISPLACEMENT AT INTERIOR SUPPORT VS TIME

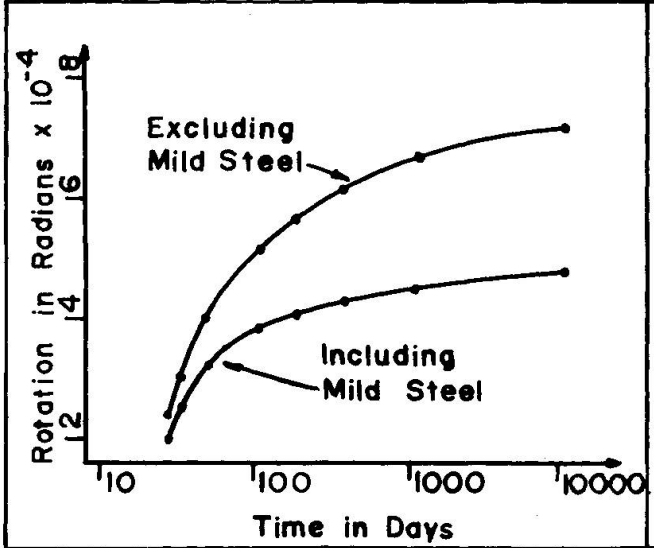

FIG. 14. ROTATION AT INTERIOR SUPPORT VS TIME

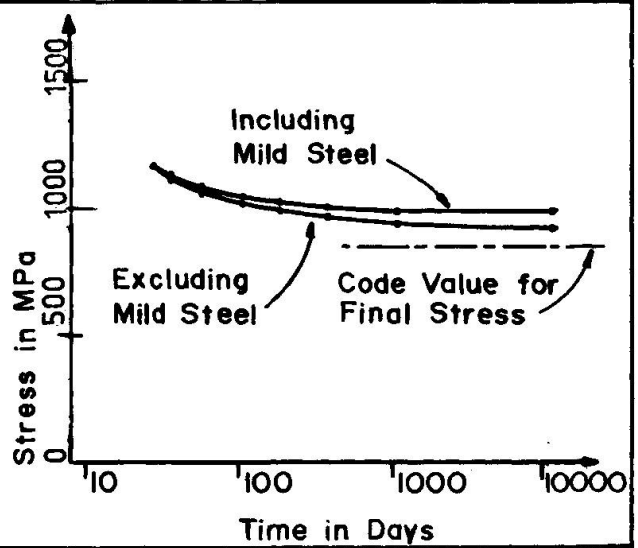

FIG. 15 TENDON STRESS AT CENTER SPAN VS TIME

4.3 Results for Prestressing Tendon Stress

Figure 15 shows variation of stress in the post tensioning strand with time, for the bridge model including nominal mild steel reinforcement as well as the model neglecting this steel. Comments pertaining to the displacement response are also applicable to this stress variation with time: most of the stress loss occurs within the first 100 days, and after 10000 days, little additional loss occurs. The figure also shows the significant discrepancy between the losses predicted by this analysis and those arrived at through AASHTO design specification [1] procedures. The finite element analysis predicts losses 25 and 40 percent lower than the AASHTO procedure, respectively, for the model without and with mild steel reinforcement. This is probably because the design specification is based on an extrapolation of data from shorter time periods and is intended to be a conservative guide to design.

4.4 Results for Curvatures

Figure 16 depicts the change in curvatures with time along the half length of the prestressed bridge model without mild steel reinforcement. Trends here are again similar to those in the displacement response: curvatures increase much more between 28 days and 300 days than in the period between 28 days and 10000 days. Note that the points of zero curvature (inflection points) move with time. Since the girder stresses remain in the elastic range throughout the time period, and since the loads on the girder do not change, the change in the distribution of curvature along the span can be attributed to the variation in loss of prestress. This is of only minor significance in the overall response.

4.5 Results for Moments

The moment diagram along the half length of the bridge is shown in Fig. 17. Moments shown include those due to applied dead load plus the so-called "secondary" prestressing moments. "Primary" prestressing moments are not included. There is only a very small redistribution of moment during the time period considered, with a slight shift of the total static moment away from the center of each span toward the interior support. This is due to the net reduction in prestressing force, and the associated reduction of the "secondary" moment.

4.6 Summary for Time Dependent Analysis

The results of this material and time dependent nonlinear analysis are in general agreement with the observed behavior of continuous post tensioned concrete box girder bridges. Time dependent deformations occur rapidly in the early stages of the history of the bridge, and then decrease markedly after several years. The presence of mild steel reinforcement stiffens the bridge, restrains creep and shrinkage deformations and reduces the associated loss of prestress. Curvatures increase in a fairly uniform fashion over the length of the girder, so that the final deflected shape of the structure is similar to the initial deflected shape, but with a greater magnitude. Prestressing losses are predicted in this time dependent and material nonlinear analysis to be smaller than the estimate of the design specification, but this does not adversely effect the safety of the structure.

5. OVERLOAD ANALYSIS AND LOADING TO ULTIMATE FAILURE

5.1 Description of Problem

In order to study the response of the bridge girder to increasing load levels up to ultimate failure, the analytical model of the bridge was subjected to

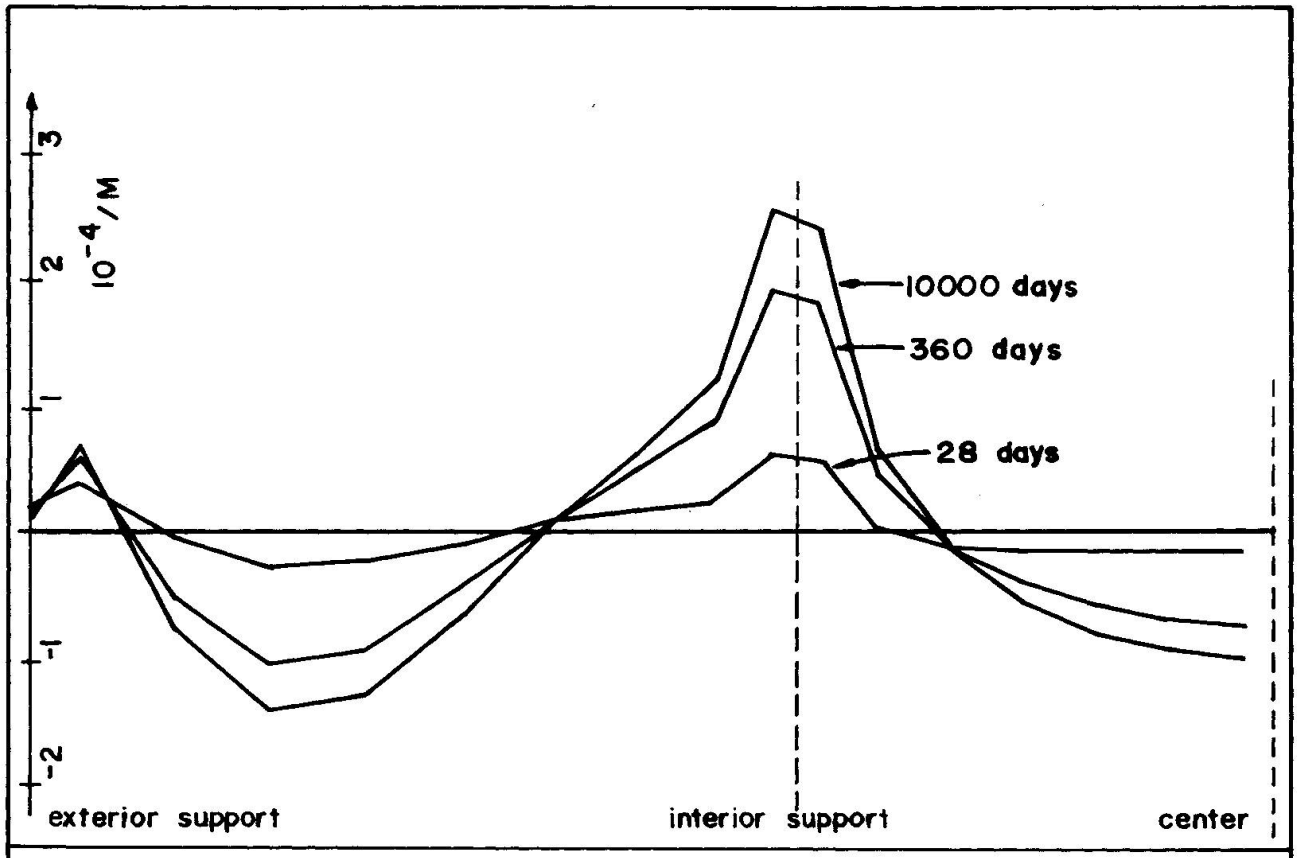

FIG. 16 CHANGE WITH TIME OF CURVATURES ALONG THE SPAN

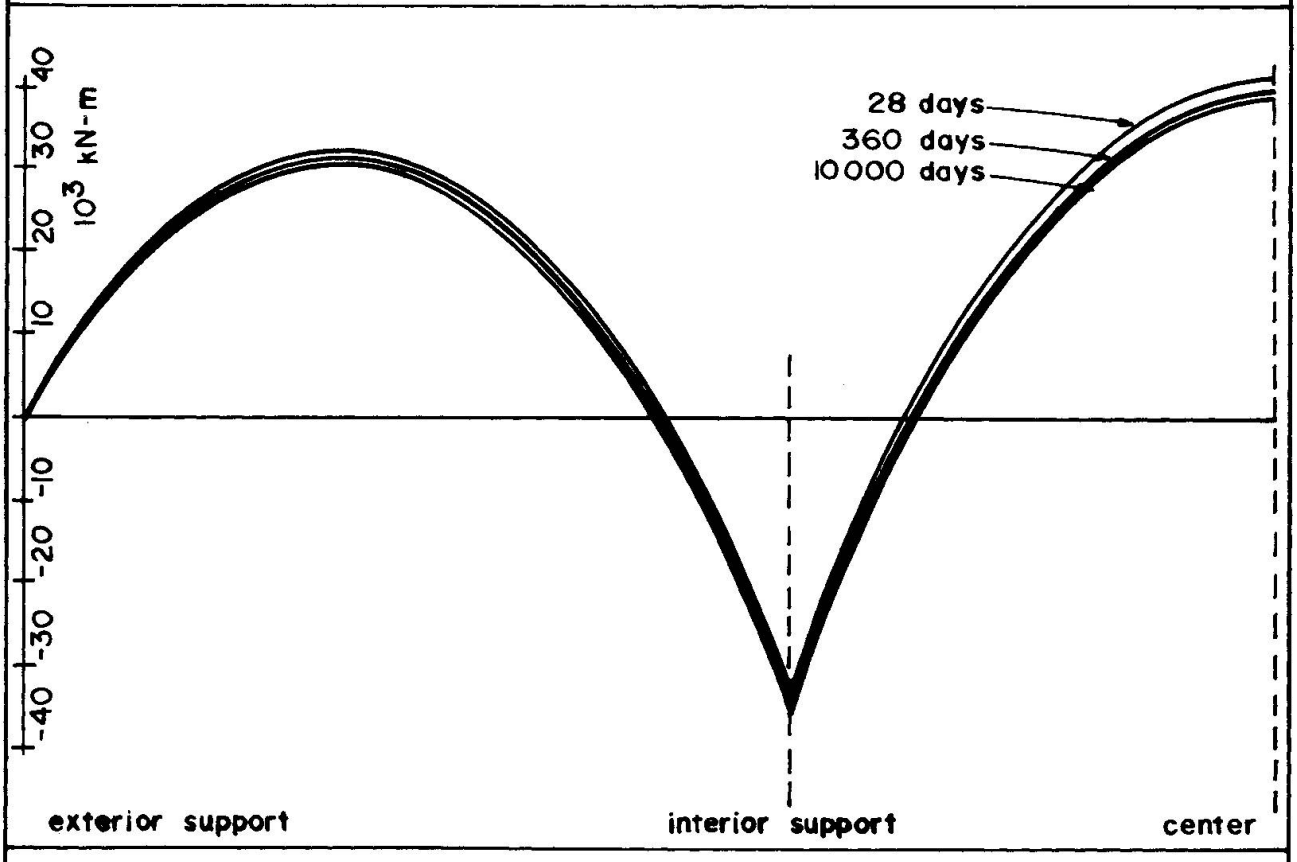

FIG. 17 CHANGE WITH TIME OF MOMENTS ALONG THE SPAN

increasing levels of vehicle overload up to ultimate failure. This analysis was carried out at two different times in relation to the time dependent analysis, once early in the history of the structure (30 days) and again late in its history (10000 days). Each analysis considers a structure previously not subjected to high overload levels. Overall response of the girder at the two loading ages proved to be quite similar, however certain differences were identified.

The overload vehicle used as a basis for the input to the analysis is typical of the heaviest vehicles found on California highways. A special road use permit is required before the vehicle is allowed on a highway, and it must travel at reduced speed. Total length of the vehicle is 33 m (108 ft), total weight is 952 kN (107 tons) and it is carried by 13 axles. In this overload analysis the truck is positioned in the middle of the center span of the bridge, and the structural load vector due to its weight is incremented until ultimate failure occurs.

The nominal mild steel reinforcement considered in the time dependent analysis is not considered in this analysis. Its ultimate capacity is very small compared with that of the post tensioning and concrete, since it is provided for construction purposes and its area is very small. The various stages of overload response are only slightly affected by the presence of this steel, and are more readily identified when it is neglected.

Multiples of the load due to one overload vehicle are incrementally applied to the analytical model in order to trace its response up to ultimate failure. At small overload levels the response of the structure is very nearly linear, so that the load increments are equal to the load due to one overload vehicle. When the total load is near the ultimate capacity of the structure, its response becomes increasingly nonlinear so that a smaller load increment equal to one fifth of the load due to one vehicle is used. This is evident in the following figures.

5.2 Results for Displacements

Figure 18 shows vertical displacement response at the center of the main span under increasing overload, for loading at both 30 days and 10000 days. The curves are of similar shape, however the structure is slightly stiffer when loaded at 30 days than when loaded at 10000 days. This is a result of the reduction in prestressing force due to time dependent effects, and the resulting decrease in cracking load of the bridge. The large overload capacity of the bridge is clearly evident in this figure. Even though service load design of the bridge is based on a load smaller than that due to one overload vehicle, so that this vehicle overstresses portions of the bridge, ultimate failure occurs at a load equal to Dead Load plus about 7.2 times the load due to one vehicle. This ultimate load level does not vary significantly with time. Simple analysis methods can be used to arrive at upper and lower bounds on the ultimate load. A lower bound solution, based on an inelastic analysis of the cross section and an elastic analysis of the girder, results in an ultimate load estimate of Dead Load plus 5 times the load due to one vehicle. An upper bound solution, based on an inelastic analysis of the cross section and an inelastic analysis of the girder assuming large plastic hinge rotation capacities, results in an ultimate load estimate of Dead Load plus 8 times the load due to one vehicle. The computer solution predicts an ultimate load capacity between these two values.

Figure 19 depicts horizontal displacement of the bridge at the interior support under increasing vehicle overload. Note that as the vehicle load increases, the center span of the bridge increases in length, due to increasing tensile strains over a large portion of the girder depth. Initial cracking loads may be identified in this figure as the load at which the response curve first becomes nonlinear: at Dead Load plus about 3 times the load of one vehicle when loaded

at 30 days, and at Dead Load plus about 2 times the load of one vehicle when loaded at 10000 days.

5.3 Results for Prestressing Tendon Stress

Figure 20 plots tendon stresses at two critical locations along the girder under increasing vehicle overload. Response is shown only for loading at 30 days. Loading at 10000 days results in curves that are similar but shifted slightly. The initiation of cracking at the critical locations is readily identified in this figure. After Dead Load plus 3 times the load of one vehicle, cracking is initiated at the center of the main span, resulting in a large increase in tendon stress at that location. After Dead Load plus 5 times the load of one vehicle, cracking is initiated over the interior support, resulting in a similarly large increase in tendon stress at that location, and a further increase in tendon stress at center span due to a redistribution of moment. Tendon stress continues to increase under increasing overload until ultimate failure of the bridge occurs due to rupture of the tendons at the center of the main span.

5.4 Results for Cross-Section Stress Distributions

Figure 21 shows stress distributions across the depth of the bridge girder at center span and at the interior support under loading to failure at 30 days. Almost all stages of structural response can be identified in this figure. The stress distribution at each location is almost linear up to a load of Dead Load plus 3 overload vehicles. Then cracking occurs at center span, the neutral axis at that location shifts upwards, and stresses increase significantly at the interior at the interior support. After a load of Dead Load plus 5 vehicles, cracking occurs over the interior support, and both sections start to respond inelastically. Further loading causes the compressive forces to be localized in the flanges of the girder, particularly at center span, until the structure fails due to rupture of the prestressing steel. The concrete never reaches its crushing strength, since in this structure with a relatively small area of prestressing steel, the steel yields first.

5.5 Summary for Overload and Ultimate Load Analysis

This nonlinear analysis demonstrates that this bridge has a large time invariant overload capacity and an ultimate failure mechanism of the same type as predicted by a typical designer's analysis. During loading to ultimate failure the individual critical cross sections of the girder experience significant inelastic deformations. Therefore the ultimate load level is higher than that predicted by present design methods used in the United States in which redistribution of moment along the length of the bridge is neglected. Thus this fully prestressed bridge designed according to standard specifications has a high overload capacity.

6. SUMMARY AND CONCLUSIONS

A nonlinear material and time dependent analysis of a three span continuous post tensioned concrete box girder bridge has been presented. The special purpose finite element computer program PCFRAME, for the nonlinear and time dependent analysis of prestressed concrete frames, was used to obtain the numerical solutions. The time dependent response of the structure was studied over a time period of 10000 days (27 years) from the time of construction. Prestressing losses were shown to be significantly lower than predicted by conventional methods. Overload response up to ultimate failure was studied both before and after the passage of time, demonstrating that the structure has a large time

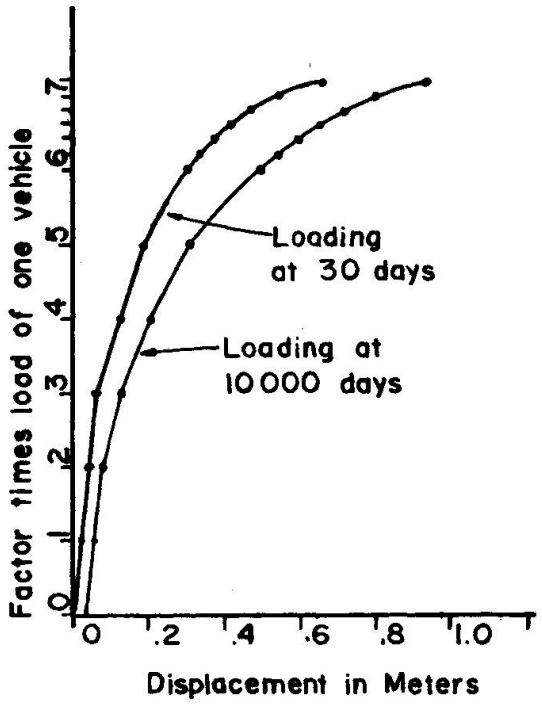

FIG. 18 VERTICAL DISPLACEMENT AT CENTER SPAN UNDER OVERLOAD

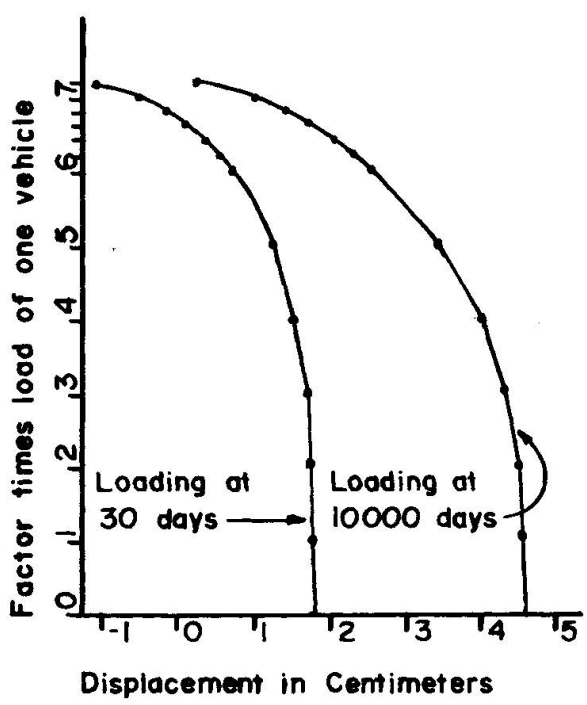

FIG. 19 HORIZONTAL DISPLACEMENT AT INTERIOR SUPPORT UNDER OVERLOAD

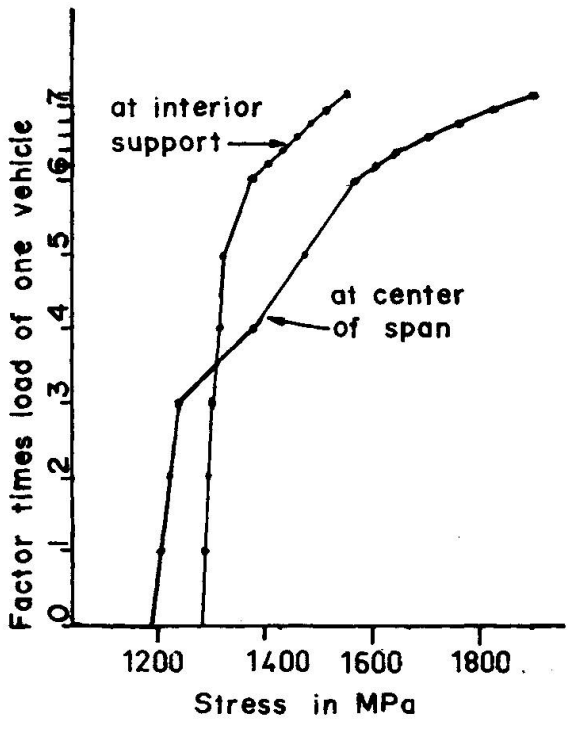

FIG. 20 TENDON STRESS AT CRITICAL SECTIONS UNDER OVERLOAD

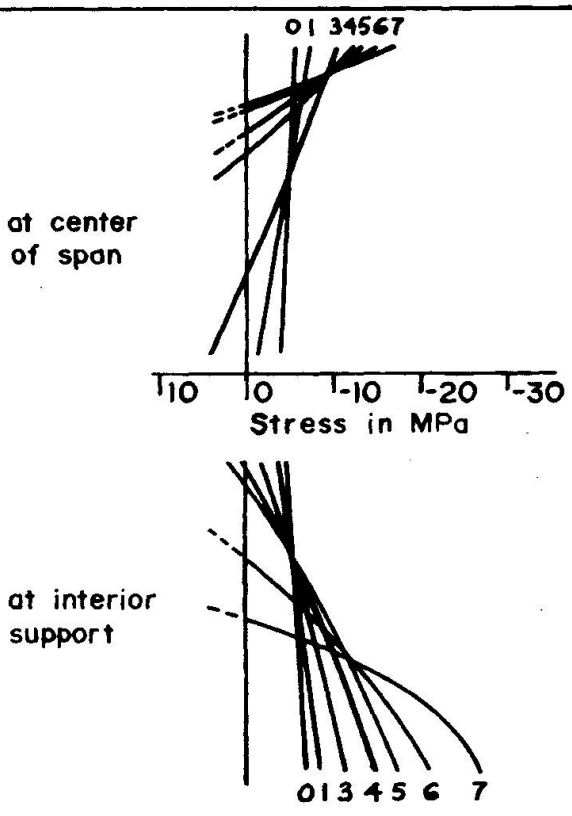

FIG. 21 STRESS DISTRIBUTION AT CRITICAL SECTIONS UNDER OVERLOAD

invariant overload capacity. Conventional methods of estimating ultimate capacity were shown to provide reasonable bounds on the total load capacity of the bridge.

Additional developments in the material, geometric, and time dependent analysis of concrete bridge structures considering segmental construction schemes as well as the three dimensional nature of the box girders are currently being carried out.

ACKNOWLEDGEMENTS

This research was partially sponsored by the U. S. National Science Foundation by Grant No. CME 7918057. The Computer Center of the University of California, Berkeley, provided the facilities for the numerical work.

REFERENCES

1. Standard Specifications for Highway Bridges, 11th Edition, American Association of State Highway and Transportation Officials, Washington, D.C., 1977.

2. CASSANO, R. C., LE BEAU, R. J., "Correlating Bridge Design Practice with Overload Permit Policy," Transportation Research Record 664, National Research Council, Washington, D.C., 1978.

3. KANG, Y. J., "Nonlinear Geometric, Material, and Time Dependent Analysis of Reinforced and Prestressed Concrete Frames," thesis presented to the University of California, Berkeley, in 1977, in partial fulfillment of the requirements for the degree of Doctor of Philosophy in Civil Engineering.

4. KANG, Y. J., SCORDELIS, A. C., "Nonlinear Analysis of Prestressed Concrete Frames," Journal of the Structural Division, ASCE, Vol. 106, No. ST2, Proc. Paper 5886, Feb. 1980.

5. HOGNESTAD, E., "A Study of Combined Bending and Axial Load in Reinforced Concrete Members," University of Illinois Engineering Experiment Station, Bulletin Series No. 399, Bulletin No. 1, 1951.

6. ACI Committee 209 (Chaired by D. E. Branson), "Designing for Effects of Creep, Shrinkage, and Temperature, ACI-SP27, American Concrete Institute, Detroit, 1971.

7. BRANSON, D. E., CHRISTIASON, M. L., "Time-Dependent Concrete Properties Related to Design Strength and Elastic Properties, Creep, and Shrinkage," SP-27, Designing for Effects of Creep, Shrinkage, and Temperature, American Concrete Institute, Detroit, 1971.

8. CEB-FIP Model Code for Concrete Structures, Commité Eurointernational du Béton-Fédération Internationale de la Précontrainte, CEB Bulletin No. 124/125-E, Paris, 1978.

9. BAZANT, Z. P., PANULA, L., "Creep and Shrinkage Characterization for Analyzing Prestressed Concrete Structures," PCI Journal, May/June 1980.

10. MUKADDAM, M. A., BRESLER, B., "Behavior of Concrete under Variable Temperature and Loading," ACI SEminar on Concrete for Nuclear Reactors, ACI-SP27, American Concrete Institute, 1972.

11. BECKER, J., BRESLER, B., "FIRES-RC, A Computer Program for the Fire Response of Structures-Reinforced Concrete Frames," Report No. UCB FRG 74-3, University of California, Berkeley, August 1974.

12. MAGURA, D. D., SOZEN, M. A., SIESS, C. P., "A Study of Stress Relaxation in Prestressing Reinforcement," PCI Journal, Vol. 9, No. 2, April 1964.

13. HERNANDEZ, H. D., GAMBLE, W. L., "Time Dependent Prestress Losses in Pretensioned Concrete Constructions," Structural Research Series No. 417, Civil Engineering Studies, University of Illinois, Urbana, May 1975.